frontiers in Energy Research

ORIGINAL RESEARCH
published: 20 October 2021
doi: 10.3389/fenrg.2021.649141

Reactive Structures of Ammonia MILD Combustion in Diffusion Ignition Processes

G. Sorrentino[1], P. Sabia[2], G. B. Ariemma[1,2], R. Ragucci[2] and M. de Joannon[2]*

[1]Dipartimento di Ingegneria Chimica, dei Materiali e della Produzione Industriale, Università degli studi di Napoli "Federico II", Naples, Italy, [2]Istituto di Scienze e Tecnologie per l'Energia e la Mobilità Sostenibili (STEMS), Consiglio Nazionale delle Ricerche (CNR), Naples, Italy

Reactive structures have been analyzed, when ammonia is used as a fuel, in a steady 1D counterflow diffusion flame layer, mimicking diffusion ignition processes. The characterization has been carried out in a wide range of feeding parameters under Moderate or Intense Low-oxygen Dilution (MILD) combustion conditions. Both the Hot-Fuel-Diluted-Fuel (HFDF) and Hot-Oxidant-Diluted-Fuel (HODF) configurations were studied to analyze the main effects of the inlet feeding conditions on the oxidative structures. The reaction zone has been analyzed in terms of temperature and heat release profiles in the mixture fraction space for various ranges of inlet parameters, using a standard code and a validated chemical kinetic scheme. Several features of the reaction zone have been recognized as reported also in previous works for hydrocarbon flames. They were used as discriminative for the achievement of various combustion regimes. In particular, the flame thickening process and the absence of correlation between the maximum heat release and the stoichiometric mixture fraction were analyzed to build maps of behaviors. The latter were reported on an inlet preheating level-temperature increase plane for fixed values of the bulk strain rate and system pressures. Another relevant feature previously reported with hydrocarbons in the literature, in Hot Diluted Diffusion Ignition (HDDI) processes under MILD conditions, was the pyrolysis depression. The latter characteristic has been not observed when ammonia is used as a fuel, for the operative conditions here investigated. Indeed, the heat release profiles do not show the presence of negative heat release regions. The results obtained for the HFDF configuration are strongly dependent on the system pressure level. Finally, the HODF condition has been also analyzed for ammonia at the atmospheric pressure. Boundaries of the combustion regimes and reactive structure features showed several differences between HFDF and HODF cases with respect to the inlet parameters.

Keywords: diffusion ignition, ammonia, MILD combustion, HFDF, HODF

OPEN ACCESS

Edited by:
Graham J. Nathan,
The University of Adelaide, Australia

Reviewed by:
Michael John Evans,
University of South Australia, Australia

****Correspondence:***
G. Sorrentino
g.sorrentino@unina.it

Specialty section:
This article was submitted to Process and Energy Systems Engineering, a section of the journal Frontiers in Energy Research

Received: *04 January 2021*
Accepted: *29 September 2021*
Published: *20 October 2021*

Citation:
Sorrentino G, Sabia P, Ariemma GB, Ragucci R and de Joannon M (2021) Reactive Structures of Ammonia MILD Combustion in Diffusion Ignition Processes. Front. Energy Res. 9:649141. doi: 10.3389/fenrg.2021.649141

INTRODUCTION

In the context of new technological solutions able of simultaneously meeting thermal efficiency needs and pollutant emission restrictions, while responding to the flexibility with respect to operating conditions and fuel properties, Moderate or Intense Low-oxygen Dilution (MILD) Combustion represents a promising solution, able to accommodate the complexity and variability of energy mix, by avoiding drastic changes in the configuration of conventional plants (Cavaliere et al., 2008).

A paradigm shift is realized in the context of such combustion systems: the process is studied as a chemical reactor, that needs to be optimized for efficiency, eco-sustainability and fuel flexibility. Oxidation process relies on local ignition phenomena due to the presence of hot gases/fresh reactants mixtures that realizes low oxygen levels (Perpignan et al., 2018). Moreover, high dilution levels prevent the stabilization of diffusive and/or deflagrative structures in an environment where self-ignition occurs. As a consequence, the reactive structure strongly differs from conventional combustion cases, showing homogeneity of temperatures and scalars inside the reactor volume, the absence of a visible flame front and reduced pollutant emissions (such as CO, nitrogen oxides and soot) (Weber et al., 2005). The oxidative regions, under highly diluted and preheated conditions, attain a distributed ignition regime with small gradients of scalar quantities (Minamoto et al., 2014). It gives the opportunity to use a broad range of fuels, being a very good candidate for low-calorific-value fuels (Huang et al., 2014), hydrogen-based and industrial wastes (Derudi and Rota, 2019), as well as for liquid (Ye et al., 2015) and solid fuels (Saha et al., 2017).

Recently, few works showed also the possibility of using carbon free fuels such as ammonia or ammonia/hydrogen blends in advanced combustion technologies with promising results (Li et al., 2019; Sorrentino et al., 2019; Valera-Medina et al., 2019; Ariemma et al., 2020).

In addition, the elementary processes that are attained in MILD conditions differ from those involved in conventional systems, due to strong overlapping between mixing and chemistry effects (Galletti et al., 2007). Flue gas entrainment induces high local diluent levels so that chemical kinetics become slow enough to operate on time scales comparable to mixing ones (Özdemir and Peters, 2001).

Reactive structures obtained under highly diluted and/or preheated reactants conditions were rigorously analyzed in the literature for laminar diffusive layers in 1D configurations (de Joannon et al., 2009, 2012) and under the occurrence of multiple mixing layers (Sorrentino et al., 2017). Part of this interest is due to the relevance of these processes in pre-chamber jet ignition (Sidey and Mastorakos, 2018) as well as in inter/intra gas turbine combustion chamber (Nemitallah et al., 2018), but mostly in furnaces, gasification (Kwiatkowski et al., 2013) and incineration applications where low-heating value fuels (Song et al., 2013) are burned in a hot products environment.

The analysis of the combustion regimes that are realized when a fuel flow is impinged toward an oxidant stream in diffusion ignition processes, has to consider all the possible boundary conditions to include MILD combustion feeding parameters. In particular, in the Hot Diluted Diffusion Ignition (HDDI) process, both the fuel and oxidant streams are diluted and pre-heated at different levels, resulting in several configurations which may lead to diverse reactive structures. Several experiments confirmed the establishment of peculiar stabilization regimes in 2D systems, mimicking hot and diluted reactive conditions (Oldenhof et al., 2010; Ye et al., 2018). In such cases the oxidation process is sustained through multiple ignition kernels that are transported by the mean flow.

Diffusion-controlled reactive structures were also characterized in laminar coflow diffusion flames, in order to investigate the salient details of non-premixed MILD combustion systems and to provide insights into the chemical structure of such regime. Comprehensive experimental and computational studies of the heat release structures and their impact on laminar flames have been carried out by different groups to characterize the main features of the oxidative regions (Abtahizadeh et al., 2013; Sepman et al., 2013; Najafi et al., 2021).

In such a framework, a systematic classification of the phenomenologies that are attained under different boundary conditions was rigorously reported in the literature (de Joannon et al., 2009; de Joannon et al., 2012).

Specifically, the Hot-Fuel-Diluted-Fuel (HFDF) feeding case, mimicked local conditions that can occur in several applications such as the coal combustion, low heating value fuel oxidation derived from processes or systems with internal flue gas recirculation systems (Kwiatkowski and Mastorakos, 2016).

Another interesting case is the Hot-Oxidant-Diluted-Fuel (HODF) configuration, that is relevant in gas turbine applications with low heating value fuels (Maruta et al., 2000) and incineration processes for the destruction of volatile organic compounds (VOC).

Such configurations were previously analyzed for low molecular weight paraffins (de Joannon et al., 2009), as well as biogas (Chen and Zheng, 2011) and hydrogen (Chen et al., 2012).

The main results of such literature works were that, in MILD combustion conditions, the reactive structures are profoundly different with respect to the ones observed in conventional diffusion flames. In particular, the heat release profiles are widened in the mixture fraction space with the simultaneous disappearance of the pyrolytic region. At the same time, the location of the oxidation region in the Z-space is not correlated to the stoichiometric mixture fraction (Z_{st}). The latter behavior is more evident in the HODF case where the reactive structure is moved toward the hot side, whereas the Z_{st} follows an opposite trend. Such oxidative structures supported the occurrence of a Diffusion-Ignition process (Sorrentino et al., 2020).

The peculiar microstructures that are realized in MILD reactive processes, are reported in the literature as "ignidiffusive structures" because they are characterized by a distributed diffusion-controlled local auto-ignition (Sorrentino et al., 2020). They revealed unconventional features of the oxidation region when high dilution and preheating levels of the reactants are established. This structure corresponds to the apparent macroscopic uniformity of the combustion and gives rise to a highly stable reactive process.

The above literature survey, concerning the categorization of the reactive structures that were obtained in diffusion ignition processes, are limited in discussing the performance of traditional fossil fuels under these novel combustion conditions. Up to date the corresponding characterization of such oxidative layers with sustainable energy carriers, such as ammonia or their blends, in innovative combustion regimes is still quite sparse. To the authors' best knowledge, until now very few papers dealt with this issue (Ku et al., 2018; Colson et al., 2020), despite they were

focused more on the extinction characteristics of ammonia flames and their blends.

Thus, the previous arguments clearly showed that the characterization of the reactive ignidiffusive structures, in highly diluted and/or preheated conditions, provides key information on the sustainability and potentiality of MILD Combustion with new fuels for several technological applications.

Although it is a promising way to utilize ammonia more in novel combustion technologies, the necessary knowledge concerning the oxidation regimes that can be reached in the utilization of such new energy vector, is highly desired before it could be widely implemented with confidence in its performance (Valera-Medina et al., 2021).

In this framework, the present work aims to extend the categorization of the reactive structures in the 1D diffusive configuration, by investigating two feeding cases corresponding to the HFDF and HODF configurations when ammonia is used as a fuel.

Such elementary process was chosen to provide a systematic classification of the phenomenologies that are attained with ammonia under MILD conditions and that were rigorously recognized in the literatures by several combustion groups with fossil fuels. Several emerging features involving dilution and preheating effects on the reactive structures can be recognized only when elementary configurations are adopted, to decouple the chemistry effects from the fluid-dynamics ones.

The investigation was performed numerically by following a similar approach to the ones that were carried out in previous papers by the same group on HODF (de Joannon et al., 2009) and HFDF (de Joannon et al., 2012) configurations. Major emphasis has been placed on the HFDF case that resembles the majority of the technological applications. For this configuration, sensitivity analysis has been carried out to show the influence of the pressure on the system reactivity.

In particular, the methodology deals with detailed numerical simulations in 1D diffusion layers where the thermochemical patterns were obtained in a large set of feeding parameters. The main combustion regimes and their boundaries are reported and the most relevant differences between the oxidative regions are investigated as a function of the process parameters. Thus, the obtained results are compared between the two different configurations and the discussion on their implications extends the conceptual framework that was previously outlined.

Diffusion ignition elementary processes mimic in a proper way the local conditions that occur in MILD burners where internal recirculation of burned products influences both on the local and global scales the ignition/oxidation patterns.

The main originality of the present work is the investigation and characterization of the reactive structures of ammonia MILD in the diffusion ignition process. It provides a systematic classification of the phenomenologies that are attained with ammonia under MILD conditions and that were rigorously recognized in the literatures by several research groups with carbon fuels.

In particular, the influences of: 1) the preheated temperature of the fuel or oxidizer flows, 2) the diluent concentration in the fuel flow, 3) the system pressure, on the oxidative structure features of ammonia under peculiar combustion conditions are investigated with the aid of numerical simulations.

It is found that the sustainability of MILD combustion, fueled with ammonia under highly diluted conditions, is highly dependent on the preheating level of the reactants and system pressure.

CONFIGURATIONS AND NUMERICAL TOOLS

The reactive structures that are attained in a steady 1D diffusion ignition process were analyzed through the opposed counter-flowing jets configuration. A sketch of the system is reported in **Figure 1** where it represents both the HFDF and the HODF.

It is worth to note that such canonical configuration aims to mimic the reactive structures that can be obtained in a real system, both on the macro and micro scales.

Specifically, a diluted ammonia-nitrogen stream (NH_3/N_2), with an inlet temperature (T_0), fuel molar fraction (X_f) and velocity (V_0) counter-diffuses toward an air jet with a certain preheating level (T_{in}). In the HFDF configuration the fuel flow is preheated at a fixed level whereas T_{in} = 300 K. On the opposite, in the HODF case T_0 = 300 K whereas T_{in} is higher than the ambient temperature. The momentum of both the streams was fixed in such a way that their kinetic energies are equals. In this manner the stagnation point is always located at the center of the mixing layer for frozen conditions, in each case here considered (Mastorakos et al., 1995). The study was carried out by means of numerical computations with OPPDIFF module of Chemkin-Pro package (CHEMKIN-PRO 15131, 2013).

Thus the boundary conditions here used were related to the inlet jets velocity (V_0, V_{in}), feeding temperatures (T_0, T_{in}) and streams mole fraction (X_f for the fuel jet and air composition for the oxidizer jet). System pressure (P) was also fixed for each computation at P = 1 Atm or 20 Atm to evaluate the effect of such parameter.

1D counterflow flame model that solves the governing equations based on a similarity solution, while neglecting buoyancy in the momentum equation, were solved in the one-dimensional physical space (Kee et al., 1989) with thermal diffusion, multi-component diffusion with species Lewis number modelled according to the transport database, and a constant imposed rate of strain, K_0. The mixture-averaged transport model was also compared with the multi-component one to verify that differences in both the thermal and chemical reactive structures were negligible.

The steady time step size was chosen to be 10^{-6} s while the relative and absolute tolerances were 10^{-5} and 10^{-9}, respectively.

Computations were tested to assure sufficient spatial resolution at the reaction zone and that solutions were independent on the grid size. The non-uniformly spaced grids of up to 250 points were found to be sufficient to resolve the reaction zone.

The bulk strain rate of the fuel flow (K_0) is equal to V_0/D.

Several reaction mechanisms reported in the literature for ammonia combustion were evaluated. In particular, Manna et al.

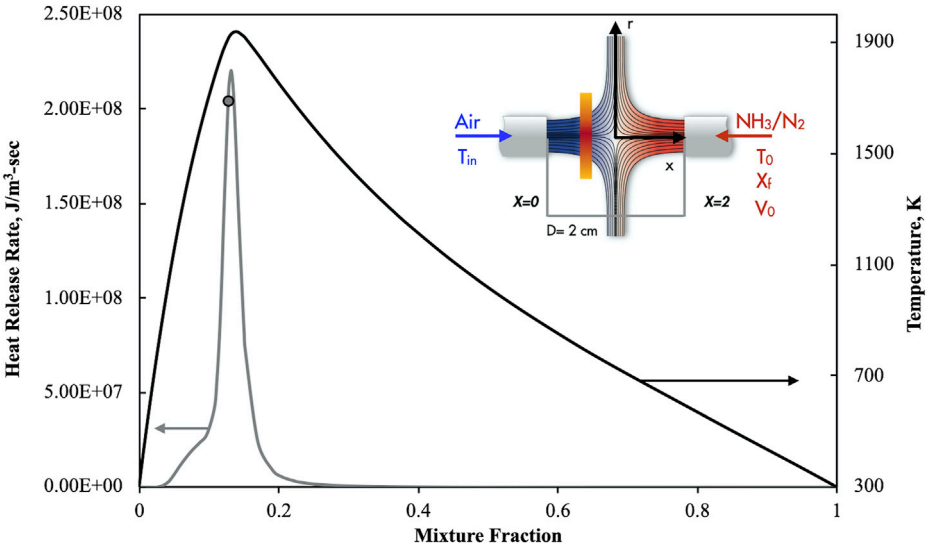

FIGURE 1 | Schematization of steady unidimensional diffusive layer configuration.

(2020) reported an experimental characterization of NH_3 oxidation and pyrolysis processes in diluted conditions in two model reactors (JSFR and LFR). The effect of several diluents, such as argon or water, were evaluated. Numerical simulations were performed with different kinetic mechanisms available in literature to value their capability to describe ammonia chemistry. In particular the authors compared the numerical results obtained with the "Konnov" (Konnov and Ruyck, 2000), "Glarborg" (Glarborg et al., 2018), "Song" (Song et al., 2016) and "Nakamura" (Nakamura et al., 2017) mechanisms. Among them the Nakamura kinetics model (Nakamura et al., 2017) was reported as the one with the best performance that predicted in a consistent way the experimental trends. Such findings were also confirmed by another work of the same research group for different dilution levels and diluents nature (Sabia et al., 2020).

The Nakamura mechanisms is a detailed kinetics (Nakamura et al., 2017) that was validated for ammonia/air on the basis of experimental tests in a micro flow reactor with controlled temperature profiles, at atmospheric pressure, at several equivalence ratios (Φ = 0.8, 1.0, 1.2) and temperatures lower than 1,400 K. The mechanism consists of 38 species and 232 reactions."

The characterization of the oxidative structures has been carried out in the manuscript by analyzing the temperature (T) and heat release rate ($\dot{h}$) profiles as a function of the mixture fraction (Z).

For conventional feeding conditions of both the air and ammonia jets (T_{in} = T_0 = 300 K with no dilution), temperatures and heat release profiles were reported in **Figure 1** with black and grey lines, respectively. In particular, when both the streams are undiluted, the system temperature (solid black line) quickly passes from 300 K (at Z = 0) up to T_{max} = 1,930 K around the stoichiometric value of Z = Z_{st} = 0.135. Subsequently, the temperature has a smooth reduction as the mixture fraction increases, attaining T_0 = 300 K at Z = 1.

The corresponding heat release trend (grey curve) sharply increases up to $\dot{h}_{max}$ that is located nearby both the T_{max} and Z_{st} values.

The $\dot{h}$ after reaching its maximum value then gradually decreases down to zero. Such profile shows the prevalence of exothermic reactions that mainly lead to the formation of intermediate or to products of oxidation.

It is very important to note that the heat release profile with pure ammonia shows only positive values, denoting for such conditions the absence of the pyrolysis region that is usually recognized with hydrocarbon flames in the richest negative heat release regions (Sidey et al., 2016). Such behavior is mainly related to the non-carbon nature of the fuel and the predominance of exothermic reactions that overcome the endothermic ones (Kobayashi et al., 2019).

Detailed numerical computations were performed over a wide range of parameters such as T_0, T_{in}, dilution of the fuel jet (X_f) and system pressure. Results were reported in the following sections for both the HFDF and HODF cases.

RESULTS AND DISCUSSION

Reactive structures in one-dimensional diffusive layer are strongly influenced by dilution and/or preheating levels of both the fuel and oxidant flows. As explained in the previous sections, two configurations were considered in this work, on the basis of the inlet streams boundary conditions. In particular, the HFDF condition referred to the case where the fuel inlet flow is diluted and preheated at fixed levels. Moreover, the effect of system pressure variation on the oxidative structures for the pure ammonia cases was also reported.

Afterwards the HODF condition was investigated at ambient pressure and for the pure ammonia case to show the main differences with respect to the HFDF case.

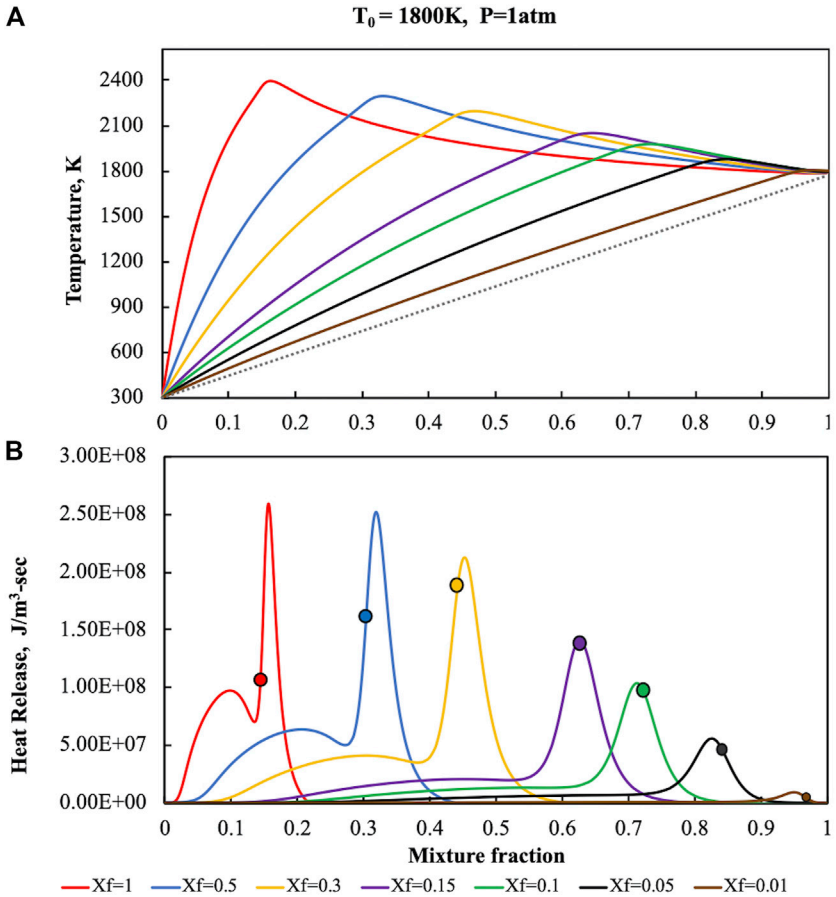

FIGURE 2 | Temperature **(A)** and heat release **(B)** profiles for pure ammonia parametric in X_f in the HFDF configuration for T_0 = 1,800 K, K_0 = 50 s^{-1}, P = 1 Atm.

Hot Fuel Diluted Fuel

The reactive structures that were obtained in the HFDF case have been reported in **Figure 2** where temperature (upper part) and heat release (lower part), numerically evaluated for a fuel pre-heating level of 1,800 K, K_0 = 50 s^{-1} and p = 1 Atm, were showed as a function of the mixture fraction on diagrams parametric in X_f, which ranges from 1 to 0.01. Solid lines represent both T and $\dot{h}$ variables and their colors change as a function of the fuel dilution level (X_f). Frozen line is also reported in the temperatures diagram with a dashed line. Solid circles in the heat release profiles indicate the stoichiometric mixture fraction (Z_{st}) values for each X_f level.

The bulk strain rate value here used (K_0 = 50 s^{-1}) was chosen in accordance with the previous studies on diffusion ignition processes with hydrocarbons from the same research group (de Joannon et al., 2009; de Joannon et al., 2012), in order to compare the results here obtained with the methane ones.

At X_f = 1, i.e., for no fuel dilution cases, the T profile is very close to the one showed for conventional conditions in **Figure 1**. In particular, due to the fuel preheating level, T values reaches a higher maximum value of 2,400 K for Z = 0.153, then decreases due to thermal diffusion. Even the heat release profile at X_f = 1 is very similar to the one obtained for the standard case. It increases up to a first relative maximum at Z = 0.089, then it attains a second absolute maximum which occurs at Z = 0.156, slightly higher than Z_{st}, that cause the enlargement of the oxidative region toward higher Z values. Afterwards the heat release decreases down to zero, thus no pyrolysis region was observed due to the absence of negative $\dot{h}$ value zones. Such behavior is mainly ascribable to the non-carbon nature of the fuel, in contrast to the prevalence of endothermic zones in some part of the heat release profile that were observed for hydrocarbons in previous works (de Joannon et al., 2012; Sorrentino et al., 2020).

Thus, oxidative structure stabilization occurs in a narrow mixture fraction region (between Z = 0.08 and Z = 0.16) that includes the two maxima where the most part of the conversion occurs.

Fuel content decrease amplifies the differences with respect to standard conditions.

For X_f = 0.5, the maximum temperature values occurs at higher mixture fractions (Z = 0.32), which is nearby to $Z_{st}^{Xf=0.5}$ = 0.305. Subsequently the temperature decrease is somewhat smoother than that observed without dilution. In particular, the maximum temperature increase is about 1,600 K, lower than 1,900 K, reached in the undiluted case. As a consequence, the oxidative region in the related heat release profile is shifted

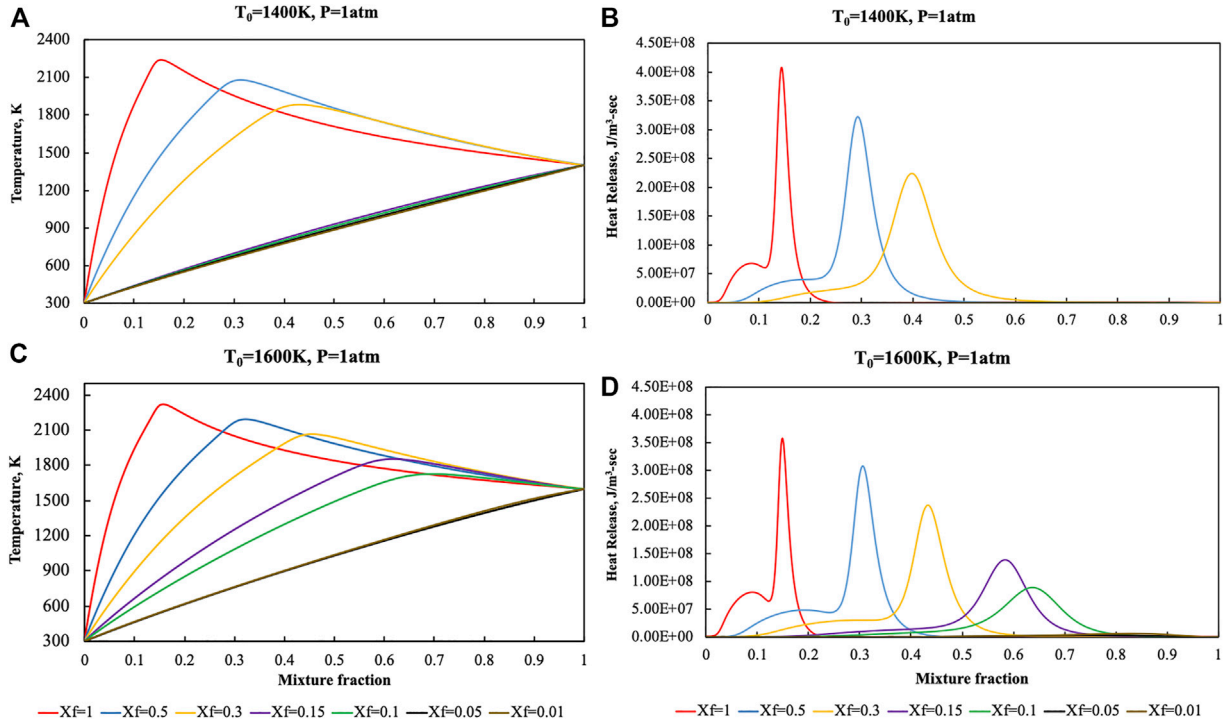

FIGURE 3 | Temperature and heat release profiles for pure ammonia parametric in X_f in the HFDF configuration for T_0 = 1,400 K **(A, B)** and T_0 = 1,600 K **(C, D)**, K_0 = 50 s^{-1}, P = 1 Atm.

and widened. When compared to the undiluted case, even in this case, two positive maxima were observed with a less pronounced shoulder at Z = 0.2.

The latest behavior is further emphasized when the dilution is increased. In fact, as reported in **Figure 2B**, the first maximum in the heat release profile disappears when X_f is decreased from 0.3 to 0.15 (purple line).

The alteration of the reactive structure becomes more complicated when the fuel dilution is further increased. The oxidative region is progressively shifted toward higher mixture fraction locations, following the shift of Z_{st} with the X_f decreasing. Specifically, two main effects of the dilution increase can be appreciated. The first one is the evolution of the left shoulder in correspondence of the first heat release maximum. The first peak results to be embedded in the remaining structure for X_f values around 0.2. At the same time, a substantial widening of the oxidation region in the Z-space occurs, by outlining a modification of the reactive structure. The dilution increasing allows to shift the region of the space where ignition occurs towards higher Z locations identified by higher frozen temperatures. $\dot{h}$ profiles maximum intensity is strongly decreased when passing from X_f = 0.3 to X_f = 0.01, in contrast to what happens for lower dilution levels (X_f > 0.3).

The preheating level of T_0 = 1,800 K was chosen as exemplificative of the different reactive structures that are achievable when ammonia content in the NH_3/N_2 mixture is decreased down to X_f = 0.01. In such a manner it is possible to analyze the oxidative structure also for very high dilution levels. Indeed, in the case of lower preheating levels (T_0 = 1,400 and T_0 = 1,600 K) such oxidative structures are not sustained for highly diluted conditions (X_f < 0.1), thus extinction occurs.

Temperature and heat release profiles were reported in **Figure 3** for lower preheating levels (T_0 = 1,400 and T_0 = 1,600 K) to show the sensitivity of the diffusion ignition process with respect to T_0.

As previously said, extinction process occurs at T_0 = 1,600 K for N_2 dilution levels higher than 90% whereas such critical value decreases to 70% when T_0 = 1,400 K.

Such kind of behaviors were recognized on the basis of both the temperature and heat release rate profiles with T values very close to the frozen line and $\dot{h}$ values that are approximately zero.

On the basis of the heat release rate (HRR) profiles, such as the one reported in **Figure 2B** or **Figures 3A,B,D** global categorization of the combustion regimes occurring under the different feeding conditions was performed, by carrying out numerical simulations in the T_0 range between 800 and 2,000 K in the whole interval of ammonia dilution (from X_f = 1 to X_f = 0.01). Such kind of analysis pursued an approach that was already followed in previous works of the same group for hydrocarbon fuels, related to HFDF and HODF feeding operative conditions (de Joannon et al., 2009). Consequently, a map of behavior for the system reactivity was achieved as a function of the inlet parameters, i.e., T_0 and X_f (fuel dilution level). The latter one is reported on the map by taking into account the maximum temperature increment ΔT for the inlet feeding conditions. Thus the map reported in **Figure 4** was obtained in the T_0-ΔT plane for

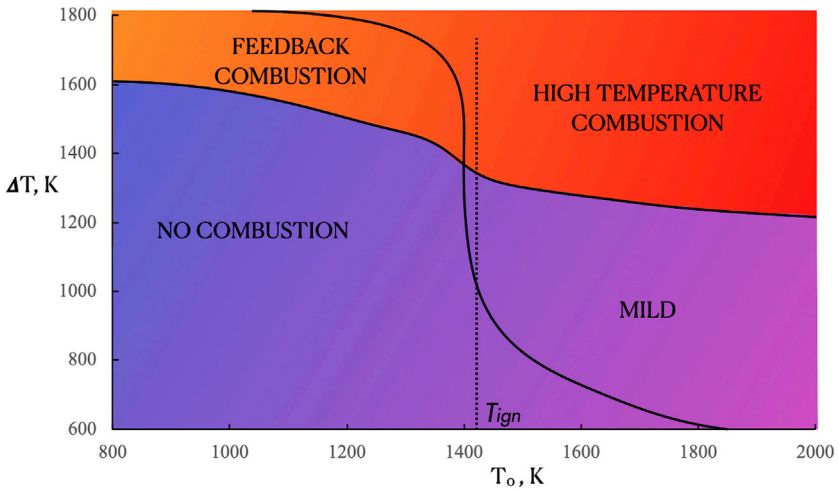

FIGURE 4 | Map of behavior for pure ammonia in the HFDF configuration at P = 1 atm.

T_{in} = 300 K, K_0 = 50 s^{-1} and p = 1 Atm. The fuel preheating temperature ranged from 800 to 2,000 K, while ΔT ranged from 600 to 1,800 K.

The map showed in **Figure 4** reported mainly four combustion regimes that are in some aspects similar to the ones obtained for methane in previous papers (de Joannon et al., 2009; de Joannon et al., 2012).

The boundaries between each zone have been obtained by investigating the shape or magnitude of heat release and/or T curves for each T_0 value. The lowest T_0 and ΔT values were obtained in the lower-left region of the map. Such zone was classified with the "No Combustion" condition, where the heat released is zero and T profiles are coincident with the frozen one in the entire range of Z values. For ΔT in the range between 850 and 1,600 K no combustion conditions were obtained up to T_0 = T_{ign}, that is the characteristic ignition temperature of ammonia at p = 1 Atm. Such regime without heat released widens up to T_0 = 1,800 K for ΔT lower than 850 K. In the T_0 interval between 800 K and T_{ign} a temperature increment (ΔT) higher than 1,600 K is able to sustain a "feedback" combustion regime, where the heat release is supported by species and heat obtained from the reaction front, such as the one detected for conventional systems. In such cases, the flame stabilization process is the one typical of diffusion flames. The region where oxidation occurs is centered close to the Z_{st} value in the heat release profile and it presents two maxima. It is worth to underline that, in contrast to hydrocarbon flames, ammonia diffusion ignition does not present pyrolytic conditions with negative heat release regions (Xiao et al., 2020).

For T_0 higher than the T_{ign} value, the feedback combustion regime gradually reaches the high temperature combustion one. In such region, the reactive region structure is broadened on a wider mixture fraction interval but they exhibit very similar features to the ones obtained in the feedback regime.

By decreasing the ΔT from the High Temperature Combustion region (i.e., by increasing the fuel dilution), a further broadening of the oxidative structure was observed and the MILD Combustion region is reached, where a single maximum is detected in the heat release profiles and the maximum temperature increment in the mixture fraction space is lower than T_{ign}. Another notable feature of the $\dot{h}$ profiles is associated with the position of $Z_{h_{max}}$ (location of the maximum $\dot{h}$ value in the Z space) with respect to Z_{st}. In particular, in the MILD regime such two values do not coincide, as shown for example by heat release profiles of **Figure 2B** for X_f < 0.15.

In this regard, the identification of MILD diffusion ignition conditions for ammonia combustion on the basis of temperature and heat release profiles appears to be more challenging with respect to hydrocarbons flames. In fact, in the latter cases MILD regimes for methane were characterized in previous works by three outstanding characteristics (de Joannon et al., 2012):

- Pyrolysis depression
- Flame thickening
- No correlation of the stoichiometric and maximum heat release conditions

They are notable signatures of the occurrence of MILD in HDDI processes (Sorrentino et al., 2020).

In this context, it is worth to note that the first characteristics (Pyrolysis depression) cannot be used for ammonia as a feature to identify the transition between conventional and MILD regimes. In fact, as stated above, the heat release profile with pure ammonia shows only positive values, denoting for such conditions the absence of the pyrolysis region that is usually recognized with hydrocarbon flames in the richest negative heat release regions. Such behavior is mainly related to the non-carbon nature of the fuel and is also strongly dependent on the bulk strain rate value.

Thus the second and the third characteristics have to be used as features that mark the transition to MILD conditions, as confirmed also by means of several DNS studies (Doan et al.,

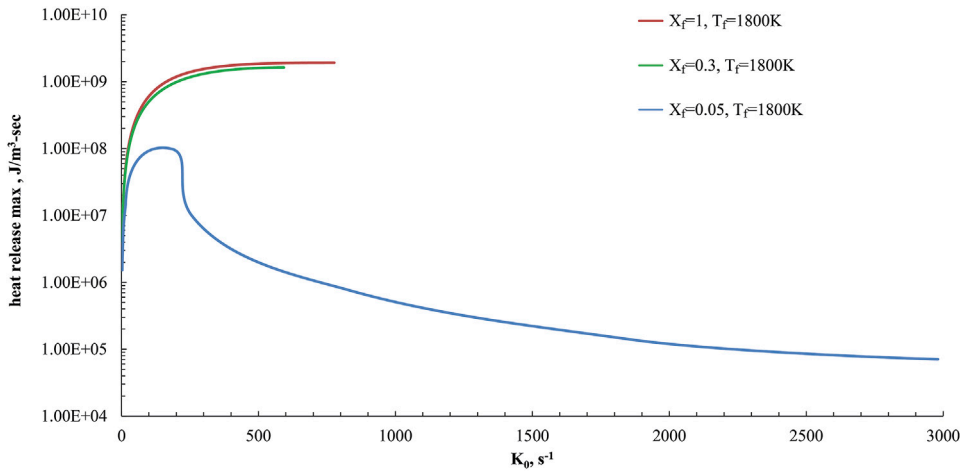

FIGURE 5 | Maximum value of the heat release profiles as a function of K_0 parametric in X_f (X_f = 1, 0.3 and 0.05) in the HFDF configuration for T_0 = 1,800 K, and P = 1 Atm.

2018; Chen et al., 2021). Besides such distinctive characteristics, MILD was also identified in this work through the temperature profiles when $\Delta T_{max}(Z) < T_{ign}$.

Another key point that needs to be remarked is that the third characteristic, i.e., the absence of correlation between Z_{st} and the maximum values of heat release, is obtained only in a limited part of the MILD domain, thereby indicating that the HDDI process is obtained in a subset of the MILD region.

The flame thickening process, related to the widening of the heat release profiles for high dilution levels ($X_f < 0.2$) marked the gradual transition of the reactive structure toward a distributed oxidation process where the "front-like" feature (Swaminathan, 2019) of the reactive region is not recognized (Ye et al., 2017).

The effect of strain rate on the reactive structures and heat release (HRR) profiles in MILD and conventional flames has been discussed in some literature works for hydrocarbon fuels (Sidey and Mastorakos, 2016). Oxidative structures are sustained under MILD conditions also at very high strain rates and, with extensive dilution and preheating, do not exhibit typical extinction behaviors (Mastorakos et al., 1995). The dissolution of an extinction strain rate in MILD conditions was already observed in previous findings for methane/air cases when reporting the heat release rate as a function of the strain rate (Sidey & Mastorakos, 2016).

Such behaviors were confirmed when ammonia is used as a fuel in the present study. In particular, numerical simulations were performed for the HFDF conditions of **Figure 2**, by changing the bulk strain rate value (K_0) and evaluating the maximum value of the heat release rate in the mixture fraction space (heat release max).

Simulations were reported in **Figure 5** for T_f = 1,800 K and three X_f values. X_f = 1 and X_f = 0.3 are related to cases in the high temperature combustion zone of the map in **Figure 4**, with a reactive region structure that is very close to a conventional combustion case. On the other hand, the case at X_f = 0.05 is related to a MILD condition, as reported previously.

The peak value of HRR for each case at varying bulk strain rates is shown in **Figure 5** as a function of K_0. Remarkable differences in the extinction behaviors between the cases at X_f = 1, X_f = 0.3 and the MILD one (X_f = 0.05) are evident.

The reactive structures at fuel mole fraction of 1 or 0.3 cannot stabilize at strain rates above 800 s^{-1} whereas the MILD one, as seen in **Figure 5**, depicted a continuous transition from high to low values of the max HRR and do not show evidence of abrupt extinction behaviors.

MILD conditions showed considerable heat released also for strain rates higher than the conventional ones and they do not extinguish up to 3,000 s^{-1}. Such features confirmed a strong extinction resilience of MILD regimes.

At very low strain rate values (lower than 25 s^{-1}), the negative heat release region appears for fuel preheating levels higher than 1,500 K, suggesting a transition from MILD to conventional combustion behavior, due to the absence of the pyrolysis depression feature as reported above.

Particularly, the minimum heat release rate becomes zero at a strain rate of 10 s^{-1} for T_f = 1,500 K whereas it is 18 s^{-1} at T_f = 1,600 K and 23 s^{-1} for T_f = 1,800 K. Those results of the heat release profiles at very low strain rate values are not presented here for brevity.

The modifications of primary kinetic pathways between the different regimes reported above in **Figure 4** were investigated by evaluating the temperature sensitivity to reaction rates as a function of the distance for two X_f values (1 and 0.01) and T_f = 1,800 K. In particular in **Figure 6** the temperature sensitivity coefficients are reported for the undiluted condition (X_f = 1) and a highly diluted case (X_f = 0.01). The latter condition is related to a MILD combustion case whereas the former pertains to a conventional combustion regime.

Results of temperature sensitivity in **Figure 6A** quantitatively demonstrate how sensitive temperature is to the reaction rate of the reaction $H+O_2=O+OH$ (branching reaction) that has the largest positive sensitivity coefficient,

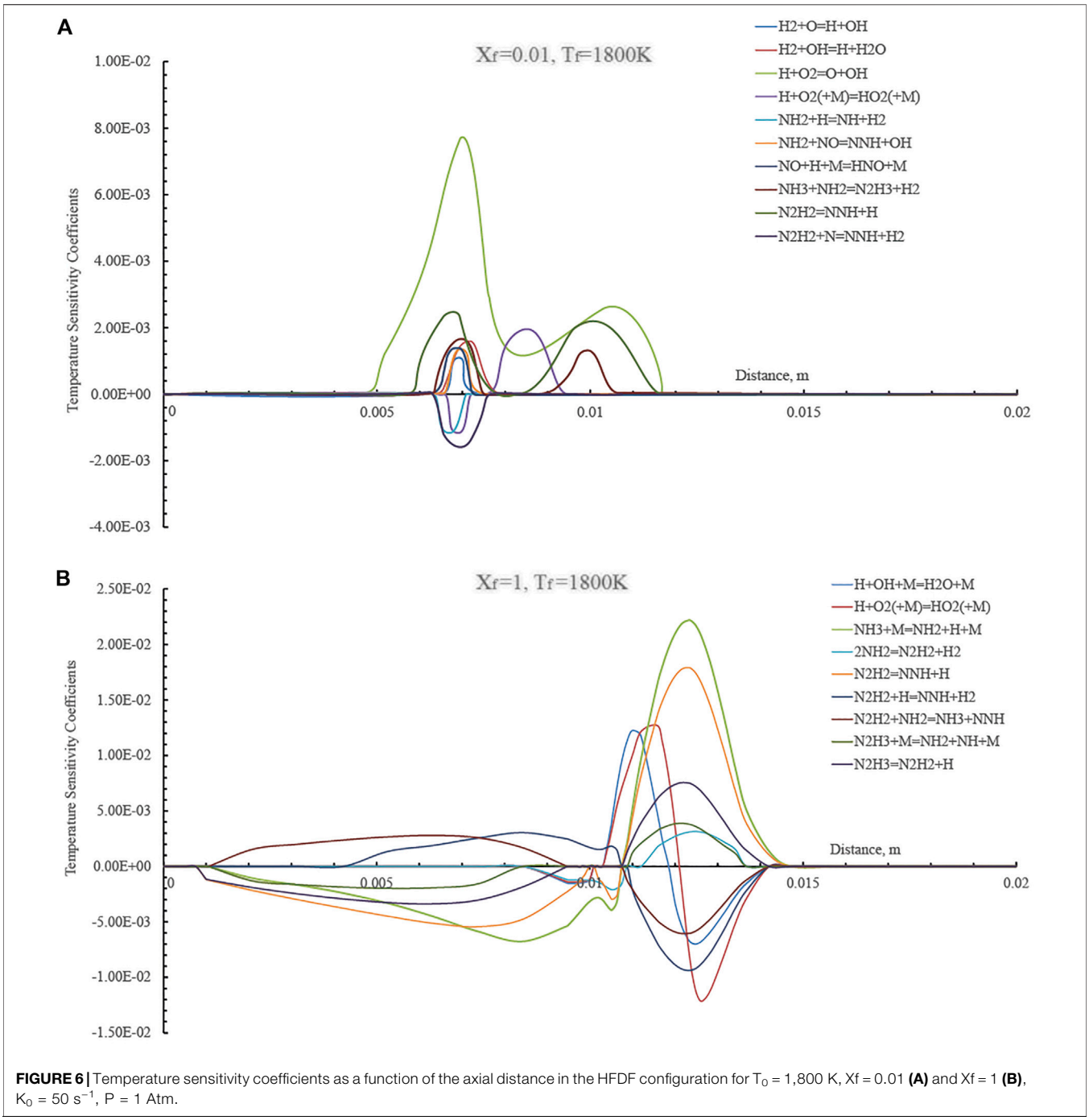

FIGURE 6 | Temperature sensitivity coefficients as a function of the axial distance in the HFDF configuration for T_0 = 1,800 K, Xf = 0.01 **(A)** and Xf = 1 **(B)**, K_0 = 50 s^{-1}, P = 1 Atm.

indicating the largest effect on increasing the temperature of the system. Reaction N_2H_2+N=NNH+H_2 has the largest negative sensitivity coefficient and affects the temperature decrease the most.

The temperature sensitivity analysis reflects strong differences between the X_f = 0.01 and the undiluted case (X_f = 1). As shown in **Figure 6B**, reaction H+O_2=O+OH no longer has the largest positive impact on temperature. In the conventional combustion case, temperature is mostly influenced by fuel-specific reactions such as the following ones: NH_3+M=NH_2+H+M and N_2H_2=NNH+H. Such results suggest that the chemical pathways of ammonia in diffusion ignition processes show different features in the various cases and provide some motivations behind the different reactive structures that were observed when passing from undiluted to highly diluted ammonia streams.

Effect of the System Pressure on Pure Ammonia

The reactive structure characterization for pure ammonia, previously obtained at P = 1 Atm, was carried out numerically

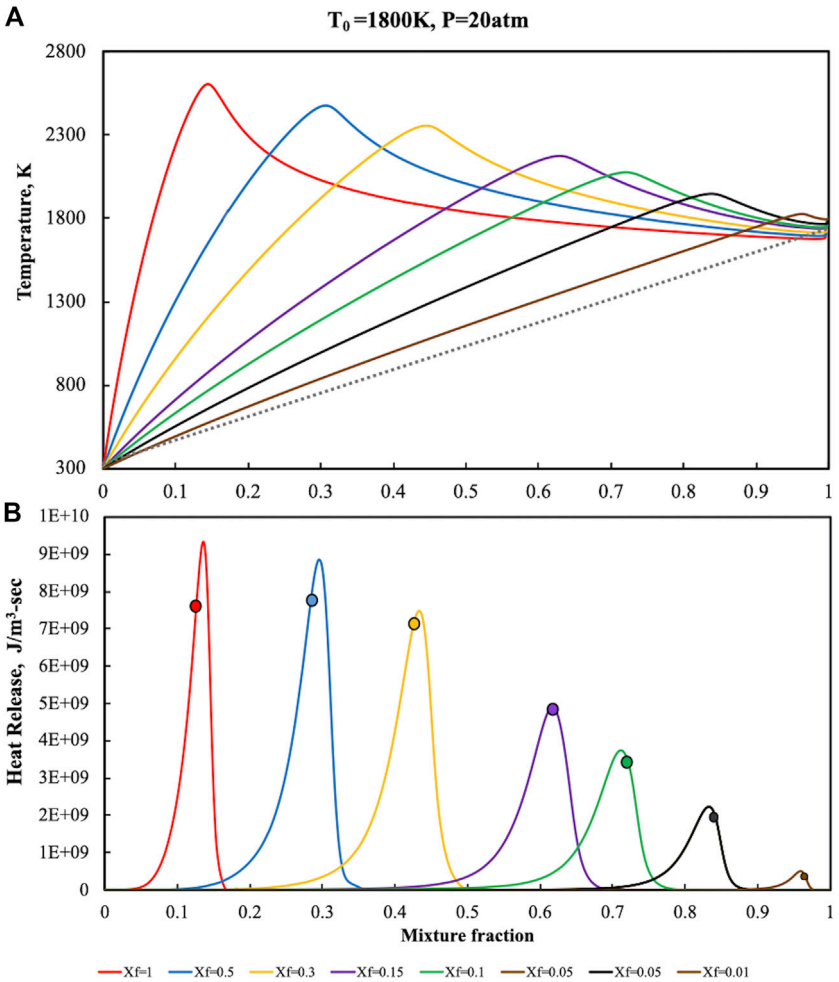

FIGURE 7 | Temperature **(A)** and heat release **(B)** profiles for pure ammonia parametric in X_f in the HFDF configuration for T_0 = 1,800 K, K_0 = 50 s^{-1}, P = 20 Atm.

also for a high pressure condition (P = 20 Atm) to show the pressure effect on the system reactivity.

In particular, as reported in **Figure 7**, Temperature and heat release profiles retain their main characteristics, even if slight differences are achieved when compared to results previously reported in **Figure 2** for T_0 = 1,800 K and K_0 = 50 s^{-1}. At 20 Atm, temperature profiles exhibit similar trends to the ones obtained at 1 Atm by showing slightly higher T values. The main differences are obtained in the heat release profiles, showing always a single maximum when the system is operated at 20 Atm. This feature can be also recognized at P = 10 Atm but such results were not reported here for brevity.

Another relevant characteristics of the reactive structure can be revealed from the heat release intensity which is almost two order of magnitude higher for P = 20 Atm with respect to the atmospheric cases.

The signatures of MILD Combustion previously identified, i.e., flame thickening and absence of correlation between Z_{st} and heat release, are also in this case attained for X_f < 0.15 when dilution levels are very high.

As showed for the atmospheric pressure case, no correlation between the stoichiometric mixture fraction and $Z_{h_{max}}$ was achieved only in a narrow subset of the MILD region.

Slight differences at higher pressures were also observed with regard to reactive structures broadening. In particular, at P = 20 Atm the heat release profiles exhibit slightly thinner oxidation structures than the ones at atmospheric conditions. This kind of behaviour is mainly related to the shortening of the chemical time scale at higher pressure levels with higher Damköhler numbers for fixed dilution levels, also in MILD conditions. Reverse-flow configurations that were investigated in the literature (Kruse et al., 2015) reported similar behaviors of the Damkohler number at higher pressures in MILD conditions. In this case the diffusion ignition process is realized locally in the burner, due to the dependence the oxidant mole fractions on both the feedings conditions and recirculation levels.

Such results that were obtained with ammonia in a simple 1D configuration can provide useful insights on the application of MILD Combustion to higher pressures (Lückerath et al., 2008)

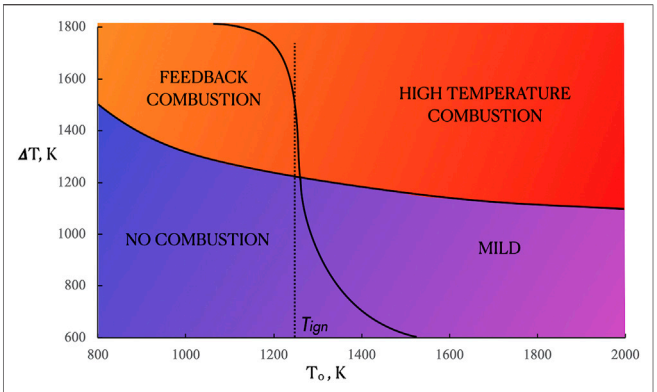

FIGURE 8 | Map of behavior for pure ammonia in the HFDF configuration at P = 20 atm.

with sustainable energy carriers in gas turbine systems (Ye et al., 2015).

On the basis of the temperature and heat release profiles that were obtained with ammonia for T_0 that ranged from 800 to 2,000 K, a map of combustion regimes for P = 20 Atm is shown in **Figure 8**. It distinctly reports that the ranges of feeding conditions that correspond to the various oxidation regions is modified to some extent while maintaining the features of the four main regimes.

By comparing the map at P = 20 Atm of **Figure 8** with the case at ambient pressure, showed in **Figure 4**, some differences can be pointed out concerning the extension of the combustion regimes. Specifically, an enlargement of both the feedback and high temperature combustion zones at higher pressures is obtained in the T_0-ΔT plane. Such behavior is mainly ascribable to both the lowering of the ignition temperature and increasing of the Damköhler number at high pressures (Khalil et al., 2019). On the other hand, both the No Combustion and MILD regimes shrink in the ΔT (i.e., fuel dilution) space.

Hot Oxidant Diluted Fuel

MILD combustion features show relevant modification in the reactive structures, with respect to the HFDF case, when diffusion ignition occurs in a mixing layer where the diluted fuel diffuses into the non-diluted hot oxidizer. Results in this section have been reported for the HODF configuration when ammonia is used as fuel, at atmospheric system pressure. Reactive structures in the HODF case have been obtained to point out the main combustion features and their differences with respect to the HFDF ones.

In the HODF configuration both the air pre-heating and the fuel dilution levels are key parameters in altering the oxidative structures as a function of their magnitude. In such a case, system temperatures (upper part) and heat release rates (lower part) were showed in **Figure 9**. In accordance with the HFDF results reported in *Hot Fuel Diluted Fuel* section, they were computed for an oxidant pre-heating temperature (T_{in}) of 1,800 K, V_0 = 100 cm/s and p = 1 Atm. T and $\dot{h}$ profiles were reported as a function of the mixture fraction and each curve is related to a fixed value of X_f, which ranges from 1 to 0.05. Both the temperature and heat release profiles are illustrated with solid lines with different colors as a function of X_f. On the same figure, frozen temperature is reported with a dashed line whereas solid circles represent the Z_{st} location pertaining to a specific X_f. When no dilution is taken into account (X_f = 1) the temperature profile that was obtained exhibits a similar aspect to the one attained under conventional conditions in **Figure 1**, albeit different magnitudes for temperatures and $\dot{h}$ values were observed.

In particular, due to the preheating, T attains a maximum value of 2,620 K for Z = 0.16, then steeply decreases toward the frozen line.

The heat release profile at X_f = 1 has an abrupt increase up to first relative maximum at Z = 0.08, then it increases in the direction of a second absolute maximum which occurs at Z = 0.16, marginally higher than $Z_{st}^{Xf=1}$ = 0.141.

Such circumstances imply a slight enlargement of the oxidation zone toward higher Z with a subsequent decrease of the $\dot{h}$ profile down to zero. Also in this case, as noted in the HFDF case, no pyrolysis behaviors were observed in the heat release profile, in contrast with the presence of pyrolytic zones obtained with hydrocarbon fuels.

The dilution of the fuel flow emphasizes the differences with respect to conventional conditions. For X_f = 0.5 the T_{max} values are moved toward higher mixture fraction (Z = 0.308), nearby the $Z_{st}^{Xf=0.5}$ = 0.305. The consequent temperature decrease is very smooth toward the frozen line when compared to what happens with no dilution. As a result, the reactive structure associated with the $\dot{h}$ profile is moved and broadens. It again shows two positive maxima with the first shoulder that has a very small maximum intensity at Z = 0.173.

The dilution increasing points out complex behaviors related to the oxidative structure evolution. In particular, at X_f = 0.3 (purple curve), the first heat release peak disappears and is embedded in the remaining structure whereas the second one broadens and is shifted toward higher Z values.

T_{max} values follows a similar behavior of those related to the heat release, revealing the maximum temperatures increment at higher mixture fractions. Another relevant effect related to the dilution increase is the location of the maximum heat release intensity with respect to Z_{st}. Specifically, for X_f = 0.3, $Z_{h_{max}}$ is lower than Z_{st} (Z = 0.43).

Fuel dilution levels higher than 70% (i.e., X_f than 0.3) lead to a different behavior of the oxidative structure that moves in the opposite direction with respect to the Z_{st} increase with the dilution.

In particular, $Z_{h_{max}}$ = 0.398 at X_f = 0.4, whereas $Z_{st}^{Xf=0.2}$ = 0.5. At the same time the heat release profile broadens and widens and its maximum intensity is moved toward the hot side (preheated air). For higher dilution levels (X_f = 0.15), the stoichiometric mixture fraction is located outside the oxidation region, as clearly showed by the $\dot{h}$ profiles for X_f = 0.15 (black curve).

The absence of correlation between the reactive structure location and the stoichiometric mixture fraction is further emphasized with the dilution level increasing, i.e., X_f < 0.15, showing a profoundly difference in the oxidative structure when compared to diffusive combustion. The latter feature, together

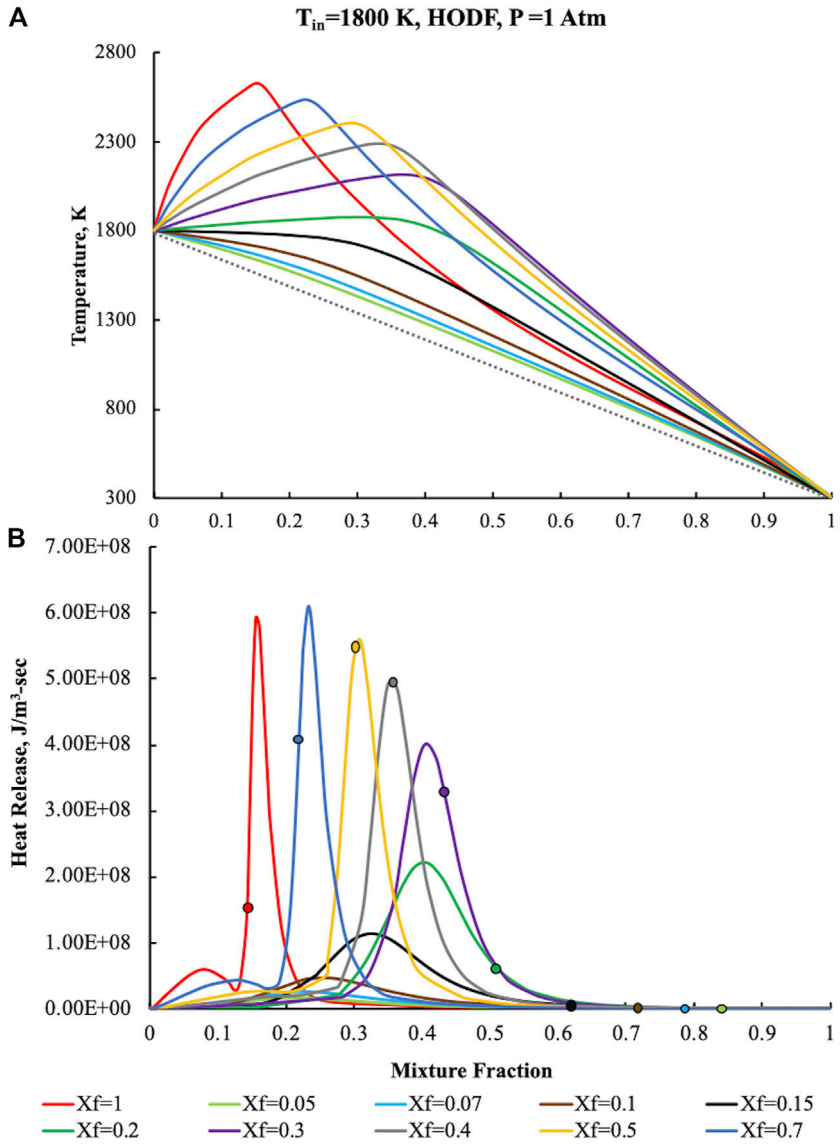

FIGURE 9 | Temperature **(A)** and heat release **(B)** profiles for pure ammonia, parametric in X_f, in the HODF configuration for T_{in} = 1,800 K, K_0 = 50 s^{-1}, P = 1 Atm.

with the broadening of the oxidation layer entail the occurrence of MILD Combustion conditions.

On the ground of the previous analysis, it is worth to note that the different characteristics of both the temperatures and heat release rate profiles are related to diverse oxidation regimes that occur as a function of the feeding parameters. They are very useful in obtaining an exhaustive categorization of the ammonia diffusion ignition process, through a map of behavior on a T_{in}-ΔT plane, where the ΔT values are directly related to the fuel dilution levels. In accordance with the previous results reported in *Hot Fuel Diluted Fuel* section for the HFDF, the map was obtained for K_0 = 50 s^{-1} and p = 1 Atm. Fuel is fed at ambient temperature whereas T_{in} was varied from 800 to 2,000 K. Ignition temperature is also reported with a dashed line (T_{ign}).

The combustion regimes map of **Figure 10** identifies four main zones. The lower left part describes the "no combustion" region, where the temperatures and residence times of the inlet two jets do not permit the achievement of a stable oxidation regime. For very low dilution levels ($X_f > 0.5$) and $T_{in} < 1{,}400$ K, the "feedback combustion" zone describe conditions where conventional diffusion flames are stabilized, i.e., the maximum reactivity is located nearby the stoichiometric conditions.

Furthermore, the upper right part of the map bounded the "high temperature combustion" zone, where very high T_{max} values are obtained because of the air pre-heating. In such a case the reactive structures are very similar to the one obtained under the feedback combustion mode. In both the regions only the oxidative region is identified in the $\dot{h}$ profiles whereas no

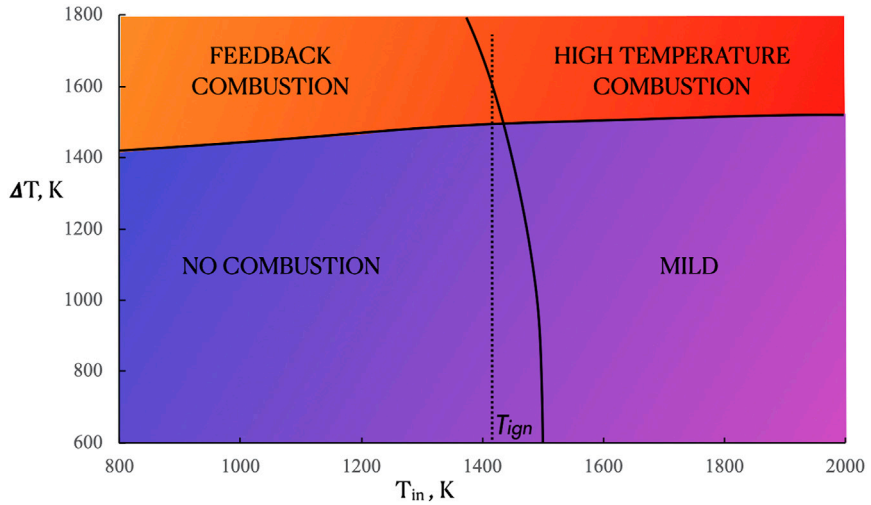

FIGURE 10 | Map of behavior for pure ammonia in the HODF configuration at P = 1 atm.

pyrolytic zones are detected. In such cases the heat release shows two maxima in the oxidative region.

Finally, the "MILD" region occurs for T_{in} > 1,500 K and X_f values lower than 0.4 (ΔT < 1,450 K) and it delineated conditions for which distributed features of the oxidation layer are recognized. Specifically, in such regime a broadening process of the heat release profile is visible in the Z-space and the maximum heat release rate occurs at Z values very low with respect to the stoichiometric ones, in contrast to what happens in both the feedback and high temperature regions.

As a final remark it is worth to underline the main differences between HFDF and HODF configurations for ammonia combustion at P = 1 Atm.

In both the cases the feedback combustion region is quite narrow, including inlet temperatures lower than 1,400 K. Similar behaviors were obtained also for the no combustion zone that is slightly wider for the HFDF case. Conversely, the high temperature combustion region is wider for the HFDF case than that under Hot-Oxidant-Diluted-Fuel conditions. Indeed, in the latter configuration, the MILD region is broadened for higher ΔT values when compared with the HFDF one. This means that MILD conditions are stabilized for lower fuel dilution levels when the oxidant flow is preheated with respect to the fuel preheating configuration.

CONCLUSION

The present study reported a categorization of the steady oxidative structures that occurred when ammonia is used as a fuel in diffusion ignition processes. The methodological approach here used was similar to that followed in previous works with hydrocarbon fuels.

The article provided a systematic classification of the phenomenologies that are attained with ammonia under MILD conditions and that were rigorously recognized in the literatures by several research groups with carbon fuels. Up to date the characterization of oxidative layers with sustainable energy carriers, such as ammonia or their blends, in MILD combustion regimes is still quite sparse. To the authors' best knowledge, until now very few papers dealt with this issue.

As a general consideration, it is important to note that the ammonia diffusion ignition process, in both the HFDF and HODF configurations, showed similar results and extend the ones obtained with hydrocarbons in previous literature studies, thus implying that the feeding parameters are reasonable choices for the obtainment of MILD combustion.

Moreover, it showed peculiar features that diversify the occurrence of MILD Combustion with ammonia with respect to fossil fuels.

Maps of behavior were obtained on the basis of the oxidative structure peculiarities that were recognized from temperature and heat release profiles. Such regime maps corresponds to local conditions that may be established in MILD combustion chambers. Specifically, inlet temperature of fuel or oxidizer flows and maximum temperature increment (i.e., the inlet dilution level of the fuel) were used as main feeding parameters to classify the combustion regimes and identify the inlet reactants conditions. Four main regions were identified in the T_0-ΔT plane as a function of both the temperature and heat release profile features.

Relevant differences in the reactive structures were obtained by comparing the HFDF results for pure ammonia at higher pressure with those achieved at atmospheric pressure.

In particular, at P = 20 Atm an enlargement of both the feedback and high temperature combustion zones was revealed with respect to P = 1 Atm. Conversely, both the No Combustion and MILD regimes shrink in the ΔT space. It means that the stabilization of MILD regimes at higher pressures requires lower minimum preheating levels but higher minimum dilution levels.

Finally, a comparison between the HFDF and HODF configurations for NH_3 combustion was carried out. In the HFDF case the High temperature combustion zone is wider than that under HODF conditions. Furthermore, in the latter configuration, the MILD part widens for higher ΔT values when compared with the HFDF one. The main information derived

from such analysis is that MILD conditions can be stabilized for lower fuel dilution levels when the oxidant flow is preheated, with respect to the fuel preheating case.

The characterization of the reactive ignidiffusive structures, in highly diluted and/or preheated conditions, provided key information on the sustainability and potentiality of MILD Combustion with new fuels for several technological applications.

DATA AVAILABILITY STATEMENT

The original contributions presented in the study are included in the article/Supplementary Material, further inquiries can be directed to the corresponding author.

AUTHOR CONTRIBUTIONS

Sorrentino and Ariemma were involved in the bibliographic research to include in the manuscript the most important literature contributions on the diffusion ignition process in MILD Combustion. They have also strongly contributed in writing several parts of the article. Sabia and de Joannon gave their support in the theoretical background regarding categorization and classification of MILD Combustion processes. Ragucci gave important insights and hints in the physical description of diffusion ignition and its connection with dimensionless numbers. He also strongly revised the English language in the manuscript.

REFERENCES

Abtahizadeh, E., Sepman, A., Hernández-Pérez, F., van Oijen, J., Mokhov, A., de Goey, P., et al. (2013). Numerical and Experimental Investigations on the Influence of Preheating and Dilution on Transition of Laminar Coflow Diffusion Flames to Mild Combustion Regime. *Combustion and Flame* 160 (11), 2359–2374. doi:10.1016/j.combustflame.2013.05.020

Ariemma, G. B., Sabia, P., Sorrentino, G., Bozza, P., de Joannon, M., and Ragucci, R. (2021). Influence of Water Addition on MILD Ammonia Combustion Performances and Emissions. *Proc. Combustion Inst.* 38, 5147–5154. doi:10.1016/j.proci.2020.06.143

Cavaliere, A., Joannon, M. d., and Ragucci, R. (2008). Highly Preheated Lean Combustion. *Lean Combust*, 55–94. doi:10.1016/B978-012370619-5.50004-2

CHEMKIN-PRO 15131 (2013). *Reaction Design*. San Diego, 2013.

Chen, S., Mi, J., Liu, H., and Zheng, C. (2012). First and Second Thermodynamic-Law Analyses of Hydrogen-Air Counter-flow Diffusion Combustion in Various Combustion Modes. *Int. J. Hydrogen Energ.* 37, 5234–5245. doi:10.1016/j.ijhydene.2011.12.039

Chen, S., and Zheng, C. (2011). Counterflow Diffusion Flame of Hydrogen-Enriched Biogas under MILD Oxy-Fuel Condition. *Int. J. Hydrogen Energ.* 36 (23), 15403–15413. doi:10.1016/j.ijhydene.2011.09.002

Chen, Z. X., Iavarone, S., Ghiasi, G., Kannan, V., D'Alessio, G., Parente, A., et al. (2021). Application of Machine Learning for Filtered Density Function Closure in MILD Combustion. *Combustion and Flame* 225, 160–179. doi:10.1016/j.combustflame.2020.10.043

Colson, S., Hirano, Y., Hayakawa, A., Kudo, T., Kobayashi, H., Galizzi, C., et al. (2020). Experimental and Numerical Study of NH3/CH4 Counterflow Premixed and Non-premixed Flames for Various NH3 Mixing Ratios. *Combustion Sci. Techn.*, 1–18. doi:10.1080/00102202.2020.1763326

de Joannon, M., Sabia, P., Sorrentino, G., and Cavaliere, A. (2009). Numerical Study of Mild Combustion in Hot Diluted Diffusion Ignition (HDDI) Regime. *Proc. Combustion Inst.* 32, 3147–3154. doi:10.1016/j.proci.2008.09.003

de Joannon, M., Sorrentino, G., and Cavaliere, A. (2012). MILD Combustion in Diffusion-Controlled Regimes of Hot Diluted Fuel. *Combustion and Flame* 159, 1832–1839. doi:10.1016/j.combustflame.2012.01.013

Derudi, M., and Rota, R. (2019). 110th Anniversary: MILD Combustion of Liquid Hydrocarbon-Alcohol Blends. *Ind. Eng. Chem. Res.* 58, 15061–15068. doi:10.1021/acs.iecr.9b02374

Doan, N. A. K., Swaminathan, N., and Minamoto, Y. (2018). DNS of MILD Combustion with Mixture Fraction Variations. *Combustion and Flame* 189, 173–189. doi:10.1016/j.combustflame.2017.10.030

Galletti, C., Parente, A., and Tognotti, L. (2007). Numerical and Experimental Investigation of a Mild Combustion Burner. *Combustion and Flame* 151 (4), 649–664. doi:10.1016/j.combustflame.2007.07.016

Glarborg, P., Miller, J. A., Ruscic, B., and Klippenstein, S. J. (2018). Modeling Nitrogen Chemistry in Combustion. *Prog. Energ. Combustion Sci.* 67, 31–68. doi:10.1016/j.pecs.2018.01.002

Huang, M., Zhang, Z., Shao, W., Xiong, Y., Liu, Y., Lei, F., et al. (2014). Effect of Air Preheat Temperature on the MILD Combustion of Syngas. *Energ. Convers. Manage.* 86, 356–364. doi:10.1016/j.enconman.2014.05.038

Kee, R. J., Miller, J. A., Evans, G. H., and Dixon-Lewis, G. (1989). A Computational Model of the Structure and Extinction of Strained, Opposed Flow, Premixed Methane-Air Flames. *Symp. (International) Combustion* 22 (1), 1479–1494. doi:10.1016/S0082-0784(89)80158-4

Khalil, H. M., Eldrainy, Y. A., Abdelghaffar, W. A., and Abdel-Rahman, A. A. (2019). Increased Heat Transfer to Sustain Flameless Combustion under Elevated Pressure Conditions - a Numerical Study. *Eng. Appl. Comput. Fluid Mech.* 13 (1), 782–803. doi:10.1080/19942060.2019.1645737

Kobayashi, H., Hayakawa, A., Somarathne, K. D. K. A., and Okafor, E. C. (2019). Science and Technology of Ammonia Combustion. *Proc. Combustion Inst.* 37 (1), 109–133. doi:10.1016/j.proci.2018.09.029

Konnov, A. A., and Ruyck, J. D. (2000). Kinetic Modeling of the thermal Decomposition of Ammonia. *Combustion Sci. Techn.* 152 (1), 23–37. doi:10.1080/00102200008952125

Kruse, S., Kerschgens, B., Berger, L., Varea, E., and Pitsch, H. (2015). Experimental and Numerical Study of MILD Combustion for Gas Turbine Applications. *Appl. Energ.* 148, 456–465. doi:10.1016/j.apenergy.2015.03.054

Ku, J. W., Choi, S., Kim, H. K., Lee, S., and Kwon, O. C. (2018). Extinction Limits and Structure of Counterflow Nonpremixed Methane-Ammonia/air Flames. *Energy* 165, 314–325. doi:10.1016/j.energy.2018.09.113

Kwiatkowski, K., Dudyński, M., and Bajer, K. (2013). Combustion of Low-Calorific Waste Biomass Syngas. *Flow Turbulence Combust* 91 (4), 749–772. doi:10.1007/s10494-013-9473-9

Kwiatkowski, K., and Mastorakos, E. (2016). Regimes of Nonpremixed Combustion of Hot Low-Calorific-Value Gases Derived from Biomass Gasification. *Energy Fuels* 30, 4386–4397. doi:10.1021/acs.energyfuels.5b02580

Li, J., Huang, H., Deng, L., He, Z., Osaka, Y., and Kobayashi, N. (2019). Effect of Hydrogen Addition on Combustion and Heat Release Characteristics of Ammonia Flame. *Energy* 175, 604–617. doi:10.1016/j.energy.2019.03.075

Lückerath, R., Meier, W., and Aigner, M. (2008). FLOX Combustion at High Pressure with Different Fuel Compositions. *J. Eng. Gas Turbines Power* 130 (1), 1–7. doi:10.1115/1.2749280

Manna, M. V., Sabia, P., Ragucci, R., and de Joannon, M. (2020). Oxidation and Pyrolysis of Ammonia Mixtures in Model Reactors. *Fuel* 264, 116768. doi:10.1016/j.fuel.2019.116768

Maruta, K., Muso, K., Takeda, K., and Niioka, T. (2000). Reaction Zone Structure in Flameless Combustion. *Proc. Combustion Inst.* 28, 2117–2123. doi:10.1016/S0082-0784(00)80621-9

Mastorakos, E., Taylor, A. M. K. P., and Whitelaw, J. H. (1995). Extinction of Turbulent Counterflow Flames with Reactants Diluted by Hot Products. *Combustion and Flame* 102, 101–114. doi:10.1016/0010-2180(94)00252-N

Minamoto, Y., Swaminathan, N., Cant, R. S., and Leung, T. (2014). Reaction Zones and Their Structure in MILD Combustion. *Combustion Sci. Techn.* 186, 1075–1096. doi:10.1080/00102202.2014.902814

Najafi, S. B. N., van Oijen, J. A., Levinsky, H. B., and Mokhov, A. V. (2021). (Non) Equilibrium of OH and Differential Transport in MILD Combustion: Measured

and Computed OH Fractions in a Laminar Methane/Nitrogen Jet in Hot Coflow. *Energy Fuels* 35 (8), 6798–6806. doi:10.1021/acs.energyfuels.1c00583

Nakamura, H., Hasegawa, S., and Tezuka, T. (2017). Kinetic Modeling of Ammonia/air Weak Flames in a Micro Flow Reactor with a Controlled Temperature Profile. *Combustion and Flame* 185, 16–27. doi:10.1016/j.combustflame.2017.06.021

Nemitallah, M. A., Rashwan, S. S., Mansir, I. B., Abdelhafez, A. A., and Habib, M. A. (2018). Review of Novel Combustion Techniques for Clean Power Production in Gas Turbines. *Energy Fuels* 32 (2), 979–1004. doi:10.1021/acs.energyfuels.7b03607

Oldenhof, E., Tummers, M. J., Van Veen, E. H., and Roekaerts, D. J. E. M. (2010). Ignition Kernel Formation and Lift-Off Behaviour of Jet-In-Hot-Coflow Flames. *Combustion and Flame* 157 (6), 1167–1178. doi:10.1016/j.combustflame.2010.01.002

Özdemir, İ. B., and Peters, N. (2001). Characteristics of the Reaction Zone in a Combustor Operating at Mild Combustion. *Experiments in Fluids* 30, 683–695. doi:10.1007/s003480000248

Perpignan, A. A. V., Gangoli Rao, A., and Roekaerts, D. J. E. M. (2018). Flameless Combustion and its Potential towards Gas Turbines. *Prog. Energ. Combustion Sci.* 69, 28–62. doi:10.1016/j.pecs.2018.06.002

Sabia, P., Manna, M. V., Cavaliere, A., Ragucci, R., and de Joannon, M. (2020). Ammonia Oxidation Features in a Jet Stirred Flow Reactor. The Role of NH2 chemistryThe Role of NH2 Chemistry. *Fuel* 276, 118054. doi:10.1016/j.fuel.2020.118054

Saha, M., Dally, B. B., Medwell, P. R., and Chinnici, A. (2017). Effect of Particle Size on the MILD Combustion Characteristics of Pulverised Brown Coal. *Fuel Process. Techn.* 155, 74–87. doi:10.1016/j.fuproc.2016.04.003

Sepman, A., Abtahizadeh, E., Mokhov, A., van Oijen, J., Levinsky, H., and de Goey, P. (2013). Experimental and Numerical Studies of the Effects of Hydrogen Addition on the Structure of a Laminar Methane-Nitrogen Jet in Hot Coflow under MILD Conditions. *Int. J. Hydrogen Energ.* 38 (31), 13802–13811. doi:10.1016/j.ijhydene.2013.08.015

Sidey, J. A. M., Giusti, A., and Mastorakos, E. (2016). Simulations of Laminar Non-premixed Flames of Kerosene with Hot Combustion Products as Oxidiser. *Combustion Theor. Model.* 20, 958–973. doi:10.1080/13647830.2016.1201146

Sidey, J. A. M., and Mastorakos, E. (2018). Pre-chamber Ignition Mechanism: Simulations of Transient Autoignition in a Mixing Layer between Reactants and Partially-Burnt Products. *Flow Turbulence Combust* 101 (4), 1093–1102. doi:10.1007/s10494-018-9960-0

Sidey, J. A. M., and Mastorakos, E. (2016). Simulations of Laminar Non-premixed Flames of Methane with Hot Combustion Products as Oxidiser. *Combustion and Flame* 163, 1–11. doi:10.1016/j.combustflame.2015.07.034

Song, F., Gu, L., Zhu, N., and Yuan, H. (2013). Leaching Behavior of Heavy Metals from Sewage Sludge Solidified by Cement-Based Binders. *Chemosphere* 92 (4), 344–350. doi:10.1016/j.chemosphere.2013.01.022

Song, Y., Hashemi, H., Christensen, J. M., Zou, C., Marshall, P., and Glarborg, P. (2016). Ammonia Oxidation at High Pressure and Intermediate Temperatures. *Fuel* 181, 358–365. doi:10.1016/j.fuel.2016.04.100

Sorrentino, G., Cavaliere, A., Sabia, P., Ragucci, R., and de Joannon, M. (2020). Diffusion Ignition Processes in MILD Combustion: A Mini-Review. *Front. Mech. Eng.* 6 (10), 1–8. doi:10.3389/fmech.2020.00010

Sorrentino, G., de Joannon, M., Sabia, P., Ragucci, R., and Cavaliere, A. (2017). Numerical Investigation of the Ignition and Annihilation of CH4/N2/O2 Mixtures under MILD Operative Conditions with Detailed Chemistry. *Combustion Theor. Model.* 21 (1), 120–136. doi:10.1080/13647830.2016.1220624

Sorrentino, G., Sabia, P., Bozza, P., Ragucci, R., and de Joannon, M. (2019). Low-NOx Conversion of Pure Ammonia in a Cyclonic Burner under Locally Diluted and Preheated Conditions. *Appl. Energ.* 254, 113676–113677. doi:10.1016/j.apenergy.2019.113676

Swaminathan, N. (2019). Physical Insights on Mild Combustion from Dns. *Front. Mech. Eng.* 5 (59), 1–8. doi:10.3389/fmech.2019.00059

Valera-Medina, A., Amer-Hatem, F., Azad, A. K., Dedoussi, I. C., de Joannon, M., Fernandes, R. X., et al. (2021). Review on Ammonia as a Potential Fuel: From Synthesis to Economics. *Energy Fuels* 35, 6964–7029. doi:10.1021/acs.energyfuels.0c03685

Valera-Medina, A., Gutesa, M., Xiao, H., Pugh, D., Giles, A., Goktepe, B., et al. (2019). Premixed Ammonia/hydrogen Swirl Combustion under Rich Fuel Conditions for Gas Turbines Operation. *Int. J. Hydrogen Energ.* 44, 8615–8626. doi:10.1016/j.ijhydene.2019.02.041

Weber, R., Smart, J. P., and Kamp, W. v. (2005). On the (MILD) Combustion of Gaseous, Liquid, and Solid Fuels in High Temperature Preheated Air. *Proc. Combustion Inst.* 30, 2623–2629. doi:10.1016/j.proci.2004.08.101

Xiao, H., Lai, S., Valera-Medina, A., Li, J., Liu, J., and Fu, H. (2020). Study on Counterflow Premixed Flames Using High Concentration Ammonia Mixed with Methane. *Fuel* 275, 117902. doi:10.1016/j.fuel.2020.117902

Ye, J., Medwell, P. R., Evans, M. J., and Dally, B. B. (2017). Characteristics of Turbulent N-Heptane Jet Flames in a Hot and Diluted Coflow. *Combustion and Flame* 183, 330–342. doi:10.1016/j.combustflame.2017.05.027

Ye, J., Medwell, P. R., Kleinheinz, K., Evans, M. J., Dally, B. B., and Pitsch, H. G. (2018). Structural Differences of Ethanol and DME Jet Flames in a Hot Diluted Coflow. *Combustion and Flame* 192, 473–494. doi:10.1016/j.combustflame.2018.02.025

Ye, J., Medwell, P. R., Varea, E., Kruse, S., Dally, B. B., and Pitsch, H. G. (2015). An Experimental Study on MILD Combustion of Prevaporised Liquid Fuels. *Appl. Energ.* 151, 93–101. doi:10.1016/j.apenergy.2015.04.019

Conflict of Interest: The authors declare that the research was conducted in the absence of any commercial or financial relationships that could be construed as a potential conflict of interest.

Publisher's Note: All claims expressed in this article are solely those of the authors and do not necessarily represent those of their affiliated organizations, or those of the publisher, the editors and the reviewers. Any product that may be evaluated in this article, or claim that may be made by its manufacturer, is not guaranteed or endorsed by the publisher.